Blind Estimation of Common Phase Error in OFDM and OFDMA

Gokul Sridharan and Teng Joon Lim
Electrical and Computer Engineering Department
University of Toronto, Canada
Email:gsridharan@comm.utoronto.ca, limtj@comm.utoronto.ca

***Abstract*—This paper addresses the issue of blind estimation of common phase error (CPE) in OFDM systems affected by phase noise (PHN). Common approaches to blind CPE detection detect the symbols, and estimates the phase noise in an iterative manner. An important assumption that these decision-directed algorithms make is that a majority of the symbols detected in the first iteration, while ignoring the presence of phase noise, have been detected correctly. This assumption fails to hold under scenarios of high CPE and leads to a premature error floor. In this paper we dispense with the assumption that most of the symbols have been detected correctly and instead associate with each symbol a certain probability of having been detected correctly. Through the introduction of an auxiliary binary variable that indicates whether the right decision on a symbol has been made or not, we design a new algorithm to estimate CPE. This algorithm is robust to high CPE scenarios and is able to lower the error floor seen at high SNRs.**

I. Introduction

The demand for higher data rates has led to OFDM becoming the technology of choice for next generation wireless standards such as WiMAX (Worldwide Interoperability for Microwave Access, IEEE 802.16) and LTE (3rd Generation Partnership Project Long Term Evolution, put forth by European Telecommunications Standards Institute). This has brought into focus the various implementation issues that are critical in an OFDM-based system. In particular, phase noise (PHN) is an impairment that needs special attention because unlike other impairments, it changes substantially over an OFDM frame and cannot be compensated for in the training stage. In this paper we address the issue of blind CPE estimation (i.e. without the use of pilot or training symbols) which is an important practical function in OFDMA, because then only a small number of sub-carriers may be allocated to one user, and hence it would be bandwidth-inefficient to insert pilots in every frame of every user.

PHN arises from imperfections in the frequency synthesizer that result in random fluctuations in the phase of the output signal. In this paper we assume phase noise to be a first-order auto-regressive (AR(1)) process as suggested in [1] for the IEEE 802.11g standard. The effect of PHN has been studied extensively [2]–[4]. The effect of PHN can be split into two: the rotation of all the sub carriers by a certain angle called the common phase error and the leakage of neighboring sub carriers resulting in inter carrier interference (ICI). CPE is the average of the PHN sequence spanning an OFDM symbol. In this paper we deal exclusively with blind CPE estimation which plays a critical role in the effectiveness of any other PHN compensation scheme; pilots based estimation schemes have been studied in [5]–[7]. We envision this work as a precursor to any joint PHN and symbol estimation algorithm that might be employed at the receiver, such as the one in [8].

Situations that call for blind estimation occur frequently. For example, in the WiMAX standard, one in every three symbols transmitted by a user to the base station is devoid of pilots. This motivates the need for a robust blind CPE estimator, designed explicitly to work in the absence of pilots. The crux of the algorithm suggested in this paper is the realization that not all symbols are equally prone to errors. Symbols on subcarriers that see a better channel are less susceptible to errors due to additive noise (ADN) while symbols with smaller magnitude are less susceptible to errors resulting from phase noise. By separating these two effects, we are able to derive an expression for the probability of correct detection of any symbol in an OFDM frame. This allows us to identify the most reliable symbols and use them as virtual pilots, with the aid of the bit-flipping sequential likelihood ascent search [9] algorithm.

The paper is organized as follows. Section II sets up the received signal model and discusses the consequences of phase noise on the received signal. Section III discusses the new algorithm that is developed to estimate CPE. Section IV presents the simulation results. All vectors and matrices are denoted in bold and estimates of unknown parameters are represented with a hat on top of the variable.

II. Received Signal Model

A. The received signal

In this work, we consider the detection of an OFDM symbol transmitted over a block fading frequency selective channel, where the channel stays constant over the duration of one OFDM symbol. We also assume that perfect frame synchronization, including carrier frequency recovery have been established in the training stage. We further assume that current channel conditions have been estimated during the training phase and that channel state information is available on the receiver side. Algorithms that can estimate the channel in the presence of PHN and carrier frequency offset have been presented in [10], [11]. In the data detection stage we assume that the received signal has been affected by PHN in addition to the channel and additive noise. The received signal for such a scenario in the discrete domain after appropriate sampling and removal of the cyclic prefix is given by

$$\mathbf{r} = \mathbf{FPF}^H\mathbf{Hd} + \mathbf{n} \tag{1}$$

Here, $\mathbf{F}$ is an $N \times N$ DFT matrix with the $(l,m)^{th}$ entry given by $\mathbf{F}_{lm} = (1/\sqrt{N})e^{-(2\pi j(l-1)(m-1)/N)}$, $\mathbf{P}$ is the diagonal matrix given by diag($e^{j\boldsymbol{\theta}}$) $\approx$ diag($\mathbf{1}+j\boldsymbol{\theta}$), where $\boldsymbol{\theta}$ is the PHN sequence and $\mathbf{H} = \text{diag}(\mathbf{h})$ is the channel matrix in the frequency domain. The vector $\mathbf{d}$ is the corresponding symbol sequence and $\mathbf{n}$ is complex white Gaussian noise with variance σ^2 each in the in-phase and quadrature dimensions.

The phase noise process is assumed to be an AR(1) process. Characteristics of such a process are given in [8]. Denoting the covariance matrix of a length-N sequence of PHN as $\boldsymbol{\Phi}$, it can be shown that the sample mean $\bar{\theta}$ given by

$$\bar{\theta} = \frac{1}{N}\sum_{k=1}^{N}\theta[k]. \tag{2}$$

is a zero mean Gaussian random variable with variance $\sigma^2_{\bar{\theta}} = \mathbf{1}^T\boldsymbol{\Phi}\mathbf{1}/N^2$ [11].

If one were to represent the received vector $\mathbf{r}$ as $[r_0, r_1, \ldots, r_{N-1}]^T$, then,

$$r_k = c_0 d_k h_k + \sum_{l=0, l\neq k}^{N-1} d_l h_l c_{(l-k) mod\, N} + \nu_k. \tag{3}$$

Here, the vector $\mathbf{c} = [c_0, c_1, \ldots, c_{N-1}]^T$ is given by $(1/\sqrt{N})\mathbf{F}^H\mathbf{p}$ (where $\mathbf{p} = e^{j\boldsymbol{\theta}}$) i.e. the frequency domain representation of the PHN sequence. It can be shown that $\boldsymbol{\nu}$ is an uncorrelated white noise process with $\nu_k \sim \mathcal{CN}(0, 2\sigma^2)$. Equation (3) clearly illustrates how PHN affects the received signal. Note that c_0 is the CPE i.e. $1+\frac{1}{N}\sum_{k=1}^{N}\theta[k] \approx e^{j\bar{\theta}}$ (under small angle assumption), and its effect is to rotate every received symbol by the average phase angle $\bar{\theta}$. Further, it can be shown that the ICI term is well approximated as a zero mean Gaussian random variable with variance $(\frac{1}{N}\text{tr}(\mathbf{F}^H\boldsymbol{\Phi}\mathbf{F}) - \sigma^2_{\bar{\theta}})E[|d|^2]E[|h|^2]$, where $E[|d|^2]$ is the average symbol energy and $E[|h|^2]$ is the variance of the channel gain on a sub-carrier.

B. Importance of CPE Estimation

CPE rotates the symbol constellation, and without pilots it is challenging to distinguish between the actual symbol being transmitted with a large phase error, and the neighboring symbol being transmitted with a small phase error. Therefore, even sophisticated methods such as the one proposed in [8] for PHN sequence estimation and compensation require that the CPE be known to a large extent.

If CPE and PHN are not compensated at all, then the symbol error probability will be unacceptable – for example, for the 64-QAM constellation a rotation of 9° causes a symbol error with probability 0.43 even in the absence of noise. Coupled with scenarios such as the WiMAX uplink in which some OFDM symbols contain no pilots, it is thus imperative for blind CPE estimation methods to be devised. We describe such a technique in the next section.

III. CPE ESTIMATION

A. Existing approaches to CPE estimation

Suppose S_p were to represent the set of indices corresponding to the pilots in an OFDM symbol, the ML estimate of CPE is given as (under small $\bar{\theta}$ assumption) [12]

$$\hat{\bar{\theta}}_{\text{ML}} = \Im\left(\frac{\sum_{k\in S_p} r_k(h_k d_k)^*}{\sum_{k\in S_p}|h_k d_k|^2}\right). \tag{4}$$

With prior knowledge of the statistics of PHN and ADN, we can also compute the MAP estimate to be

$$\hat{\bar{\theta}}_{\text{MAP}} = \Im\left(\frac{\sigma^2_{\bar{\theta}}\sum_{k\in S_p} r_k(h_k d_k)^*}{\sigma^2 + \sigma^2_{ICI} + \sigma^2_{\bar{\theta}}\sum_{k\in S_p}|h_k d_k|^2}\right). \tag{5}$$

If there are no pilots embedded in an OFDM symbol, then one can make a preliminary estimate of the symbols while ignoring the PHN and use these symbol estimates as virtual pilots to compute the CPE. In general, all the symbol decisions are used while estimating CPE.

B. Blind CPE estimation under detection uncertainty

Not all symbols are detected correctly in a practical scenario. Even in the high SNR regime, if the CPE exceeds a certain threshold, detection errors are likely to be made. The estimates in the previous subsection do not take this into consideration. In this section we present a more careful formulation of the CPE estimation problem.

We first introduce an auxiliary binary random vector $\mathbf{I}$. I_k, the kth entry of the vector $\mathbf{I}$ is 1 if the kth symbol has been detected correctly and is 0 otherwise. Rather than looking at estimation of $\bar{\theta}$ in isolation, we look at jointly estimating $\bar{\theta}$ and $\mathbf{I}$ as follows:

$$\begin{aligned}
(\hat{\bar{\theta}}, \hat{\mathbf{I}}) &= \arg\max_{\bar{\theta}, I}\ \text{p}(\bar{\theta}, I|\mathbf{r}, \hat{\mathbf{d}}) && (6)\\
&= \arg\max_{\bar{\theta}, I}\ \text{p}(\mathbf{r}|\bar{\theta}, \hat{\mathbf{d}}, \mathbf{I})\text{p}(\mathbf{I}, \bar{\theta}|\hat{\mathbf{d}}) && (7)\\
&= \arg\max_{\bar{\theta}, I}\ \text{p}(\mathbf{r}|\bar{\theta}, \hat{\mathbf{d}}, \mathbf{I})\text{p}(\mathbf{I}|\bar{\theta}, \hat{\mathbf{d}})\text{p}(\bar{\theta}) && (8)\\
&\approx \arg\max_{\bar{\theta}, I}\ \text{p}(\mathbf{r}|\bar{\theta}, \hat{\mathbf{d}}, \mathbf{I})\text{p}(\mathbf{I}|\hat{\mathbf{d}})\text{p}(\bar{\theta}) && (9)\\
&= \arg\max_{\bar{\theta}, I}\ \text{p}(\mathbf{r}|\bar{\theta}, \hat{\mathbf{d}}, \mathbf{I})\text{p}(\bar{\theta})\prod_{k=1}^{N}\text{p}(\mathrm{I}_k|\hat{d}_k) && (10)
\end{aligned}$$

Equation (9) follows from (8) if we treat $\bar{\theta}$ and $\mathbf{I}$ as independent variables. While this is clearly not true, it simplifies the maximization greatly. For the moment, we just assume that for any $\hat{d}_k$, the value of $\text{p}(I_k|\hat{d}_k)$ is known to us. Now, (10) can be written as

$$\begin{aligned}
(\hat{\bar{\theta}}, \hat{\mathbf{I}}) = \arg\max_{\bar{\theta}, I}\Bigg[&-w_{\mathbf{I}}\ln(2\pi(\sigma^2+\sigma^2_{ICI})) + \sum_{k=1}^{N}\ln(\text{p}(\mathrm{I}_k|\hat{d}_k))\\
&-\frac{1}{2\sigma^2_{\bar{\theta}}}(\bar{\theta})^2 - \frac{1}{2(\sigma^2+\sigma^2_{ICI})}\sum_{\{k:I_k=1\}}|y_k - (1+j\bar{\theta})h_k\hat{d}_k|^2\Bigg] && (11)\\
= \arg\max_{\bar{\theta}, I}&\left(a_{\mathbf{I}}(\bar{\theta})^2 + b_{\mathbf{I}}(\bar{\theta}) + c_{\mathbf{I}}\right) && (12)
\end{aligned}$$

where,

$$a_{\mathbf{I}} = \left[-\frac{1}{2\sigma_\theta^2} - \sum_{k=1}^{N} \frac{1}{2(\sigma^2 + \sigma_{ICI}^2)} I_k |h_k \hat{d}_k|^2 \right] \tag{13}$$

$$b_{\mathbf{I}} = \left[\sum_{k=1}^{N} \frac{1}{\sigma^2 + \sigma_{ICI}^2} I_k \Im\{(y_k - h_k \hat{d}_k)(h_k \hat{d}_k)^*\} \right] \tag{14}$$

$$c_{\mathbf{I}} = \sum_{k=1}^{N} I_k \Bigg\{ -\ln(2\pi(\sigma^2 + \sigma_{ICI}^2)) - \frac{|y_k - h_k \hat{d}_k|^2}{2(\sigma^2 + \sigma_{ICI}^2)} + \ln\left(\frac{P(I_k = 1|\hat{d}_k)}{P(I_k = 0|\hat{d}_k)} \right) \Bigg\} + \sum_{k=1}^{N} \ln\Big(P(I_k = 0|\hat{d}_k) \Big). \tag{15}$$

In (11), $w_{\mathbf{I}}$ is the weight of the vector **I**. The maximization above involves a search over the continuous parameter $\bar{\theta}$ and all possible N-tuples of the random vector **I**. This is an instance of a Mixed Integer Non Linear Problem (MINLP) and solving for the optimum in such cases is not easy. In this particular case, since the problem is convex in the continuous parameter $\bar{\theta}$ when the binary vector is held constant, there are methods that can find the optimal solution [13]. But, as pointed out in [13], such methods are computationally intensive and are not suited for real time applications. With simplicity of optimization in mind, we adopt a sequential likelihood ascent search (LAS) algorithm [9]. The algorithm can be broken down into the following steps.

1) Sort the subcarriers in decreasing order of the tolerance to CPE of the symbols $\hat{d}_k$. (CPE tolerance is discussed later).
2) Assume that the first l_0 subcarriers after sorting have been detected correctly. Typical value for l_0 can be around 4 to 8. This forces the first l_0 entries in **I** to be 1. Set all other entries in **I** to 0.
3) Find the $\bar{\theta}$ that maximizes the likelihood function in (11). Toggle the $(l_0+1)^{th}$ entry in **I** to 1 and find the $\bar{\theta}$ that maximizes (11). If the new maximum is greater than the previous maximum, fix the $(l_0+1)^{th}$ entry to 1 else set it to 0.
4) Proceed as in step 3 for all the remaining subcarriers in a sequential manner until all subcarriers are exhausted.

At the end of the above procedure, we end up with a vector **I** that gives a list of all the subcarriers that have been taken into consideration for the estimation of $\bar{\theta}$, and an estimate of $\bar{\theta}$ obtained through a local search. While this estimate of $\bar{\theta}$ might not be the optimal estimate, it is hoped that the initialization ensures that the process converges to a point very close to the global optimum.

C. Computing $p(I_k|\hat{d}_k)$

One basic assumption we make is that $|d_k| = |\hat{d}_k|$. Since phase noise only alters the phase of the transmitted symbol, this assumption holds in the regime where errors due to CPE dominate over those due to additive noise (ADN). Also, the discussion that follows only applies to constellations with square decision boundaries such as 16-QAM, 64-QAM etc. Under the above assumptions, Figure 1 illustrates the tolerance to CPE of a symbol $\hat{d}_k$ that is $|\hat{d}_k|$ distance away from the origin with the decision boundary $\mathcal{B}$ around $\hat{d}_k$ forming a square of side 's'.

We define the tolerance to CPE $\bar{\theta}_{tol}$ to be the maximum angle of rotation that a symbol can tolerate before it falls outside

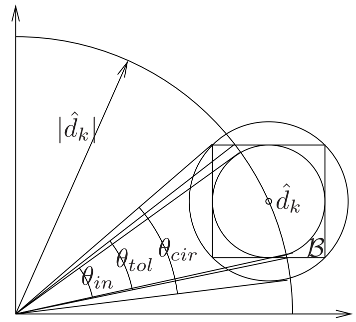

Fig. 1. Phase noise tolerance of a symbol with a square decision region.

the decision boundary. It is easy to see from Figure 1 that the tolerance to CPE of such a symbol lies between the angle subtended by the incircle (θ_{in}) and the circumcircle (θ_{cir}) of the decision region $\mathcal{B}$ at the origin. It is equal to the angle subtended by the incircle when the symbol is very close to one of the axes and is equal to the angle subtended by the circumcircle when the symbol is close to the 45°/135° lines. Hence, for a symbol that is $|\hat{\mathrm{d}}_k|$ away, one can write

$$\sin^{-1}\left(\frac{s}{2|\hat{d}_k|}\right) \le |\bar{\theta}_{\text{tol}}| \le \sin^{-1}\left(\frac{s}{\sqrt{2}|\hat{d}_k|}\right). \tag{16}$$

Note that this expression holds regardless of the value of the fading coefficient at each sub-carrier, and hence for the entire OFDM symbol. Since the effect of the channel parameter is to either shrink or expand the constellation (rotation is easily compensated), this has the same effect on both 's' as well as the distance of the symbols from the origin and hence, the CPE tolerance remains unchanged.

Now, with regard to symbol detection, the combined effect of PHN and ADN leads to four scenarios. Scenarios that lead to a correct decision include the situation where the CPE rotation is small enough to keep the transmitted symbol within the decision boundary and the ADN too is small enough to ensure correct decision. The other scenario that leads to correct decision is when the CPE is high enough to rotate the symbol to a point outside the decision boundary, but the ADN is such that it brings the received symbol back within the decision region. Let us call the former event as E_1 and the latter as E_2. Computing the probabilities P(E_1) and P(E_2) gives us the probability of correct decision. Clearly, P(E_2) is negligible in comparison to P(E_1) and

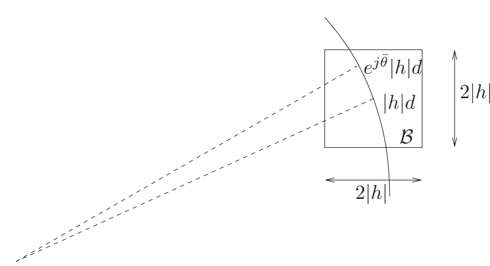

Fig. 2. Effect of PHN and ADN on a symbol

hence we focus on computing P(E_1) in the rest of this section. At this stage we would also like to introduce two classes of symbols for the convenience of the discussion that is to follow. We define a symbol to be of type I if it is on either the real or imaginary axis and type II if it is on the $45^\circ/135^\circ$ lines.

Assume that a symbol d was transmitted on a subcarrier with channel parameter h associated with it. Let Ω represent the set of all $\bar{\theta}$ that keep $|h|d$ within the decision boundary $\mathcal{B}$, then $\Omega = [-\bar{\theta}_{tol}\ \bar{\theta}_{tol}]$. Let $N_{r\bar{\theta}}$ and $N_{i\bar{\theta}}$ represent the set of values of the additive noise in the quadrature and in-phase directions that keep $e^{j\bar{\theta}}|h|d$ within $\mathcal{B}$(refer to figure (2)). We can write

$$P(E_1) = \int_{\bar{\theta}\in\Omega} P(N_{r\bar{\theta}})P(N_{i\bar{\theta}})p(\bar{\theta})d\bar{\theta} \tag{17}$$

$$= 2\int_0^{\bar{\theta}_{tol}} P(N_{r\bar{\theta}})P(N_{i\bar{\theta}})p(\bar{\theta})d\bar{\theta} \tag{18}$$

The trajectory taken by a symbol as $\bar{\theta}$ increases until it leaves the decision region $\mathcal{B}$ is dependent on the exact value of the symbol and not just its magnitude. Since the knowledge of the exact symbol is not available at the receiver, we consider two extreme trajectories, the one along a diagonal of $\mathcal{B}$ and the other along a line parallel to one of the sides and passing through the center of $\mathcal{B}$ and treat P(E_1) to be the average of the integral over these two trajectories. The first trajectory corresponds to type II symbols while the second trajectory corresponds to type I symbols. For type I symbols we set $\bar{\theta}_{\text{tol}} = \sin^{-1}\left(\frac{s}{2|\hat{d}_k|}\right)$ and for type II symbols, we set $\bar{\theta}_{\text{tol}} = \sin^{-1}\left(\frac{s}{\sqrt{2}|\hat{d}_k|}\right)$.

Since an explicit computation of the integral is not possible along either trajectory, we approximate $P(N_{r\bar{\theta}})P(N_{i\bar{\theta}})$ using linear functions. But first, we make some observations on the product $P(N_{r\bar{\theta}})P(N_{i\bar{\theta}})$. Note that for any symbol, the product $P(N_{r\bar{\theta}})P(N_{i\bar{\theta}})$ monotonically decreases as $\bar{\theta}$ increases. It takes the highest value of $K_0 = \left(1 - 2Q\left(\frac{|h|}{\sigma}\right)\right)^2$ at $\bar{\theta} = 0$ and decreases to approximately $K_2 = \left(0.5 - Q\left(\frac{2|h|}{\sigma}\right)\right)^2$ at $\bar{\theta} = \bar{\theta}_{tol}$ for type II symbols and decreases to $K_1 = \left(0.5 - Q\left(\frac{2|h|}{\sigma}\right)\right)\left(1 - 2Q\left(\frac{|h|}{\sigma}\right)\right)$ at $\bar{\theta} = \bar{\theta}_{tol}$ for a type I symbol.

Note that for a type II symbol, both, $P(N_{r\bar{\theta}})$ and $P(N_{i\bar{\theta}})$ are of the form

$$P(N_{r\bar{\theta}}) = \int_{-\frac{1}{\sigma}(|h|-\frac{1}{\sqrt{2}}|hd|\sin(\bar{\theta}))}^{\frac{1}{\sigma}(|h|+\frac{1}{\sqrt{2}}|hd|\sin(\bar{\theta}))} g(x)dx \tag{19}$$

where $g(x)$ is the standard Gaussian distribution. For type I symbols, one of $P(N_{r\bar{\theta}})$ or $P(N_{i\bar{\theta}})$ is of the above form while the other is a constant and is equal to

$$P(N_{r\bar{\theta}}) = \int_{-\frac{1}{\sigma}|h|}^{\frac{1}{\sigma}|h|} g(x)dx. \tag{20}$$

Further, note that for large $|h|$ the RHS of (19) remains almost constant over a long range of $\bar{\theta}$ until $\bar{\theta}$ equals a certain critical value of $\bar{\theta}_c$. To quantify this better we define $\bar{\theta}_c$ to be that angle below which the absolute value of the lower limit in the integral in (19) is greater than 3 standard deviations. Thus,

$$\bar{\theta}_c = \sin^{-1}\left\{\frac{\sqrt{2}}{|d|}\left(1 - \frac{3\sigma}{|h|}\right)\right\}. \tag{21}$$

Since a negative $\bar{\theta}_c$ does not makes sense, the critical angle is defined only when $|h| > 3\sigma$. Thus whenever $|h| > 3\sigma$, we can split the integral in (17) into two parts:

$$\begin{aligned} P(E_1) &= \int_{\bar{\theta}\in\Omega} P(N_{r\bar{\theta}})P(N_{i\bar{\theta}})p(\bar{\theta})d\bar{\theta} \\ &= 2\int_0^{\bar{\theta}_c} P(N_{r\bar{\theta}})P(N_{i\bar{\theta}})p(\bar{\theta})d\bar{\theta} \\ &\quad + 2\int_{\bar{\theta}_c}^{\bar{\theta}_{tol}} P(N_{r\bar{\theta}})P(N_{i\bar{\theta}})p(\bar{\theta})d\bar{\theta} \end{aligned} \tag{22}$$

Using a linear approximation to the product $P(N_{r\bar{\theta}})P(N_{i\bar{\theta}})$ in the second integral and treating the product as a constant in the first integral, for type II symbols we get,

$$P(E_1) = 2\int_0^{\bar{\theta}_c} K_0 p(\bar{\theta})d\bar{\theta} + 2\int_{\bar{\theta}_c}^{\bar{\theta}_{tol2}} \left[K_0 + \tfrac{K_2 - K_0}{\bar{\theta}_{tol2}}\bar{\theta}\right] p(\bar{\theta})d\bar{\theta} \tag{23}$$

$$= 2K_0\Big[1 - Q\left(\tfrac{\bar{\theta}_{tol2}}{\sigma_{\bar{\theta}}}\right)\Big] + \tfrac{2\sigma_{\bar{\theta}}(K_2 - K_0)}{\sqrt{2\pi}(\bar{\theta}_{tol2} - \bar{\theta}_c)}\left[e^{-\frac{\bar{\theta}_c^2}{2}} - e^{-\frac{\bar{\theta}_{tol2}^2}{2}}\right] \tag{24}$$

where $\bar{\theta}_{tol2}$ denotes the CPE tolerance of type II symbols. $\bar{\theta}_{tol1}$ is defined similarly. For type I symbols, a very similar expression can be computed by replacing $\bar{\theta}_{tol2}$ with $\bar{\theta}_{tol1}$ and K_2 with K_1. Taking the average of the two expressions, one gets

$$\begin{aligned} P(E_1) = &K_0\Big[2 - Q\left(\tfrac{\bar{\theta}_{tol1}}{\sigma_{\bar{\theta}}}\right) - Q\left(\tfrac{\bar{\theta}_{tol2}}{\sigma_{\bar{\theta}}}\right)\Big] + \\ &\sum_{j=\{1,2\}} \tfrac{\sigma_{\bar{\theta}}(K_j - K_0)}{\sqrt{2\pi}(\bar{\theta}_{tolj} - \bar{\theta}_c)}\left[e^{-\frac{\bar{\theta}_c^2}{2}} - e^{-\frac{\bar{\theta}_{tolj}^2}{2}}\right]. \end{aligned} \tag{25}$$

For scenarios where $|h| \le 3\sigma$, we do not split the integral and use a simple linear approximation over the whole interval. This gives us,

$$[P(E_1)]_j = 2K_0\Big[1 - Q\left(\tfrac{\bar{\theta}_{tolj}}{\sigma_{\bar{\theta}}}\right)\Big] + \tfrac{2\sigma_{\bar{\theta}}(K_j - K_0)}{\sqrt{2\pi}\bar{\theta}_{tolj}}\left[1 - e^{-\frac{\bar{\theta}_{tolj}^2}{2}}\right] \tag{26}$$

where $j \in \{1, 2\}$, depending on type I or type II symbol. The average, $([P(E_1)]_1 + [P(E_1)]_2)/2$ is the required probability.

Thus, depending on the channel parameter corresponding to the subcarrier, we use either (25) or (26) to compute the probability of a correct decision being made.

IV. Simulation results

To test the performance of the algorithm, we simulated a link using 64-QAM constellation and OFDM with 64 sub-carriers over a frequency selective channel. The channel was assumed to be a Rayleigh multipath fading channel with 10 taps and an exponential power delay profile. The sub-carrier spacing was set to 300 kHz. The oscillator bandwidth was set to 10 KHz and the standard deviation σ_θ was set to 3°. The MATLAB code presented in [1] was used to generate the PHN sequences.

The proposed algorithm proposed was tested along with decision-directed ML/MAP (DD-ML/DD-MAP) CPE estimation-compensation algorithms that first detect symbols

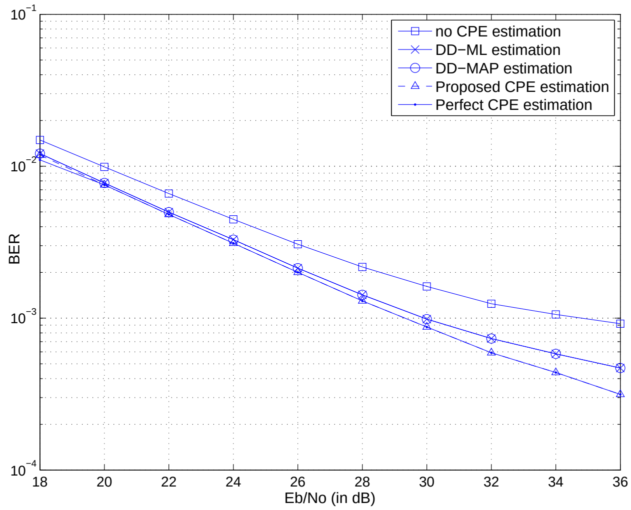

Fig. 3. BER plots for different CPE estimation schemes.

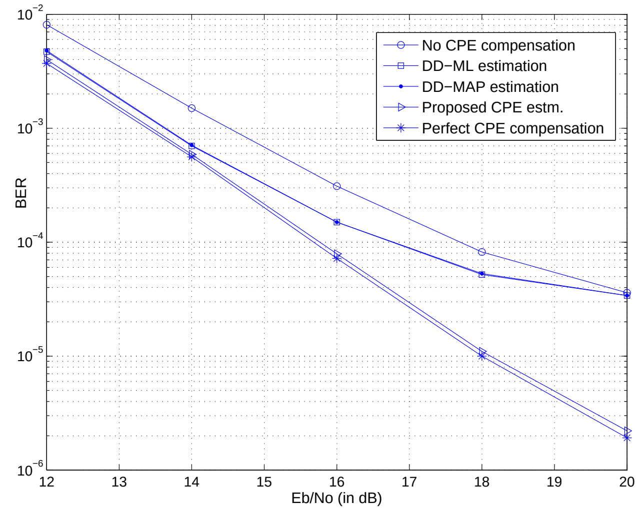

Fig. 4. BER plot of coded-OFDM with different CPE compensation schemes.

ignoring the effects of phase noise, assume no uncertainty in the symbol decisions and use them to estimate CPE. The parameter l_0 in Section III-B was set to 8 as it was found from previous simulations that a pilot driven CPE estimation with at least 8 pilots gives a good estimate of the CPE. As seen in Figure 3, while the ML and MAP estimation-compensation schemes perform almost identically, the new scheme performs much better. In fact, the curve for the proposed method is indistinguishable from the one where genie-aided CPE compensation is used. Note that there is still ICI due to the time-varying part of PHN.

In addition to the above simulations, the new scheme was also tested in a coded system. Since the SNRs of interest are much lower for a coded system it is important to test the performance of the algorithm at these SNRs, especially because the assumption in (III-C) that the magnitude of the decoded symbol and the transmitted symbol are the same need not hold at lower SNRs. Secondly, because the code is, in general, able to correct errors due to additive noise or ICI that are random in nature, frame errors are likely to arise only when the CPE estimation is not perfect and has resulted in an error burst and this gives us a better picture of the effectiveness of the proposed algorithm.

In these simulations, we used an LDPC code of rate 3/4 and length 2304, taken from the WiMAX standard. On the transmit side, the message bits were encoded, interleaved and mapped to symbols from the 64-QAM constellation. The length of the outer code was chosen so as to span 6 OFDM symbols. On the receiver side, after the reception of the 6 OFDM symbols, each was compensated for CPE and soft information was passed to the LDPC decoder. The LDPC decoder was run for 18 iterations. Figure 4 clearly shows the premature error floor resulting because of imperfect CPE estimation in the DD-ML/MAP schemes. It is seen that by using the algorithm proposed here, the error floor is no longer seen.

V. Conclusion

In this paper we highlighted the consequences of high CPE and its detrimental effect on blind decision-directed algorithms. To overcome this effect, we developed a new algorithm to estimate CPE that takes into account the reliability of symbol detection in each sub-carrier. Through simulations we have established the performance gains that can be achieved using the new scheme.

References

[1] M. Webster and M. Seals. Suggested phase noise model for 802.11hrb. [Online]. Available: https://mentor.ieee.org/802.11/dcn/00/11-00-0296-01-00sb-suggested-phase-noise-model-for-802-11-hrb.ppt

[2] T. Pollet, M. Van Bladel, and M. Moeneclaey, "BER sensitivity of OFDM systems to carrier frequency offset and Wiener phase noise," *IEEE Trans. Commun.*, vol. 43, no. 234, pp. 191–193, March 1995.

[3] D. Petrovic, W. Rave, and G. Fettweis, "Phase noise influence on bit error rate, cut-off rate and capacity of M-QAM OFDM signaling," in *In Proc. 7th Int. OFDM Workshop (InOWo)*, 2002.

[4] S. Wu and Y. Bar-Ness, "OFDM systems in the presence of phase noise: consequences and solutions," *IEEE Trans. Commun.*, vol. 52, no. 11, pp. 1988–1996, November 2004.

[5] D. Petrovic, W. Rave, and G. Fettweis, "Common phase error due to phase noise in OFDM-estimation and suppression," vol. 3, September 2004, pp. 1901 – 1905.

[6] A. Garcia Armada, "Understanding the effects of phase noise in orthogonal frequency division multiplexing (OFDM)," *IEEE Transactions on Broadcasting*, vol. 47, no. 2, pp. 153 –159, June 2001.

[7] P. Robertson and S. Kaiser, "Analysis of the effects of phase-noise in orthogonal frequency division multiplex (OFDM) systems," vol. 3, June 1995, pp. 1652 –1657 vol.3.

[8] D. D. Lin and T. J. Lim, "The variational inference approach to joint data detection and phase noise estimation in OFDM," *IEEE Trans. Signal Process.*, vol. 55, no. 5, pp. 1862–1874, May 2007.

[9] Y. Sun, "A family of likelihood ascent search multiuser detectors: an upper bound of bit error rate and a lower bound of asymptotic multiuser efficiency," *IEEE Trans. Commun.*, vol. 57, no. 6, pp. 1743 –1752, June 2009.

[10] F. Septier, Y. Delignon, A. Menhaj-Rivenq, and C. Garnier, "Monte Carlo methods for channel, phase noise, and frequency offset estimation with unknown noise variances in OFDM systems," *IEEE Trans. Signal Process.*, vol. 56, no. 8, pp. 3613–3626, August 2008.

[11] D. D. Lin, R. Pacheco, T. J. Lim, and D. Hatzinakos, "Joint estimation of channel response, frequency offset, and phase noise in OFDM," *IEEE Trans. Signal Process.*, vol. 54, no. 9, pp. 3542–3554, September 2006.

[12] K. Nikitopoulos and A. Polydoros, "Phase-impairment effects and compensation algorithms for OFDM systems," *IEEE Trans. on Commun.*, 2005.

[13] S. Leyffer, "Deterministic methods for mixed integer nonlinear programming," Ph.D. dissertation, University of Dundee, Dundee, December 1993.